

Future response of global coastal wetlands to sea-level rise

Mark Schuerch^{1,2*}, Tom Spencer², Stijn Temmerman³, Matthew L. Kirwan⁴, Claudia Wolff⁵, Daniel Lincke⁶, Chris J. McOwen⁷, Mark D. Pickering⁸, Ruth Reef⁹, Athanasios T. Vafeidis⁵, Jochen Hinkel^{6,10}, Robert J. Nicholls¹¹ & Sally Brown¹¹

The response of coastal wetlands to sea-level rise during the twenty-first century remains uncertain. Global-scale projections suggest that between 20 and 90 per cent (for low and high sea-level rise scenarios, respectively) of the present-day coastal wetland area will be lost, which will in turn result in the loss of biodiversity and highly valued ecosystem services^{1–3}. These projections do not necessarily take into account all essential geomorphological^{4–7} and socio-economic system feedbacks⁸. Here we present an integrated global modelling approach that considers both the ability of coastal wetlands to build up vertically by sediment accretion, and the accommodation space, namely, the vertical and lateral space available for fine sediments to accumulate and be colonized by wetland vegetation. We use this approach to assess global-scale changes in coastal wetland area in response to global sea-level rise and anthropogenic coastal occupation during the twenty-first century. On the basis of our simulations, we find that, globally, rather than losses, wetland gains of up to 60 per cent of the current area are possible, if more than 37 per cent (our upper estimate for current accommodation space) of coastal wetlands have sufficient accommodation space, and sediment supply remains at present levels. In contrast to previous studies^{1–3}, we project that until 2100, the loss of global coastal wetland area will range between 0 and 30 per cent, assuming no further accommodation space in addition to current levels. Our simulations suggest that the resilience of global wetlands is primarily driven by the availability of accommodation space, which is strongly influenced by the building of anthropogenic infrastructure in the coastal zone and such infrastructure is expected to change over the twenty-first century. Rather than being an inevitable consequence of global sea-level rise, our findings indicate that large-scale loss of coastal wetlands might be avoidable, if sufficient additional accommodation space can be created through careful nature-based adaptation solutions to coastal management.

Coastal wetlands provide many important ecosystem services (valued up to US\$194,000 ha⁻¹ yr⁻¹)⁹, including carbon sequestration^{10,11}, natural coastal protection^{12–15}, support of fisheries¹⁶ and water quality improvement¹⁷. Recent global-scale assessments of coastal wetland dynamics have suggested that the ability of many marshes and mangroves to build up vertically has already been overwhelmed by present-day sea-level rise (SLR), leading to widespread wetland loss^{1–3}. At the same time, more regional to local-scale field measurements and models of salt marsh accretion have concluded that most large-scale assessments have overestimated the vulnerability of coastal wetlands to SLR⁴. These differences highlight a major knowledge gap in our understanding of the responses of coastal wetland areas to global environmental change. It has been argued that the reason for the observed discrepancy is that large-scale assessments have so far failed to consider the well understood biophysical feedback mechanisms that are typically

included in local-scale models⁴. These mechanisms include the ability of coastal wetlands to build up vertically by sediment accretion, which is enhanced with increasing inundation heights and frequencies, triggered, for example, by accelerating SLR, and which enables coastal wetlands to persist or even prosper with SLR^{2–7}.

A second limitation of previous global-scale assessments is that they have not yet represented accommodation space (the vertical and lateral space available for fine sediments to accumulate and be colonized by wetland vegetation) in a spatially explicit manner^{2,4}. This constitutes an important gap, as recent papers have suggested that anthropogenic barriers to inland wetland migration (such as coastal flood protection structures, coastal roads and railway lines, settlements, and impervious land surfaces) may be a more important threat to coastal wetlands than drowning by SLR alone^{2,4,18}.

We address both of these limitations, and assess global-scale changes in coastal wetland areas in response to global SLR and anthropogenic coastal occupation, using a new integrated modelling approach. We consider (1) the vertical adaptability of coastal wetlands by biophysical feedbacks between wetland accretion and SLR, assuming current-day levels of sediment availability, and (2) their horizontal adaptability, as determined by the interactions between inland wetland migration and anthropogenic barriers, assuming wetland inland migration to be a function of accommodation space⁸. We present a model to make projections of the global resilience of coastal wetlands to twenty-first century SLR scenarios under existing and increased accommodation space, representing present conditions and two additional coastal management scenarios following the wider implementation of nature-based adaptation strategies¹². By means of a comprehensive sensitivity analysis, we finally assess the extent to which this resilience is controlled by vertical and horizontal adaptation mechanisms.

On the basis of the simulation runs during model calibration, our calibrated model, which includes mangroves as well as tidal salt and freshwater marshes, correctly predicts observations of present-day vertical wetland change, obtained from large meta-datasets from all over the world^{3,4,19}, for 78% of all coastal areas where data are currently available ($N=46$) (Extended Data Table 1, Extended Data Fig. 1). Although our model performs very well in regions where coastal wetlands were reported to be stable (that is, with vertical wetland growth in balance with local SLR) or drowning (that is, slower vertical wetland growth than local SLR), it tends to underestimate the number of locations with an elevation surplus (that is, faster vertical wetland growth than local SLR). Hence, our predictions of the ability of wetlands to vertically grow in pace with twenty-first century SLR rates may be considered conservative.

Projections of the extent of coastal wetlands by 2100 are based on simulations using three different regionalized relative SLR scenarios (Representative Concentration Pathways (RCPs) 2.6, 4.5 and 8.5,

¹Lincoln Centre for Water and Planetary Health, School of Geography, University of Lincoln, Lincoln, UK. ²Cambridge Coastal Research Unit, Department of Geography, University of Cambridge, Cambridge, UK. ³Ecosystem Management Research Group, University of Antwerp, Antwerp, Belgium. ⁴Virginia Institute of Marine Science, College of William and Mary, Gloucester Point, VA, USA. ⁵Institute of Geography, Christian-Albrechts University of Kiel, Kiel, Germany. ⁶Global Climate Forum, Berlin, Germany. ⁷UN Environment World Conservation Monitoring Centre, Cambridge, UK. ⁸Ocean and Earth Science, National Oceanography Centre, University of Southampton, Southampton, UK. ⁹School of Earth, Atmosphere and Environment, Monash University, Clayton, Victoria, Australia. ¹⁰Division of Resource Economics, Thae-Institute and Berlin Workshop in Institutional Analysis of Social-Ecological Systems (WINS), Humboldt-University, Berlin, Germany. ¹¹Faculty of Engineering and the Environment, University of Southampton, Southampton, UK. *e-mail: mschuerch@lincoln.ac.uk

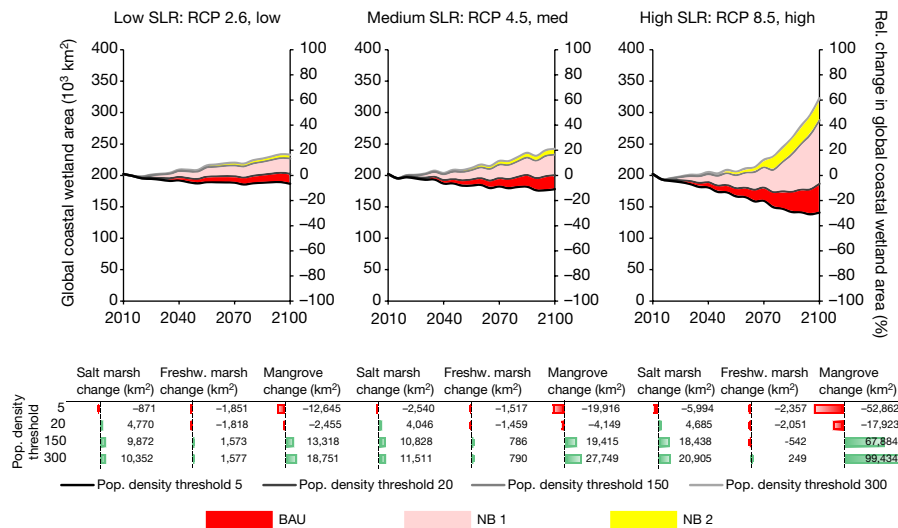


Fig. 1 | Global change in coastal wetland areas. Results are displayed for all three SLR scenarios (RCP 2.6, low; RCP 4.5, medium; RCP 8.5, high) and three human adaptation scenarios, defined by different population density thresholds (BAU 1: 5–20 people km⁻², NB 1: 20–150 people km⁻², NB 2: 150–300 people km⁻²). Sediment accretion is considered,

corresponding to an SLR of 29, 50 and 110 cm, respectively, by 2100) and three human adaptation scenarios with varying degrees of available accommodation space (Extended Data Table 2): (i) a business-as-usual (BAU) scenario, in which we assume that no accommodation space is available where local population densities in the 1-in-100-year coastal floodplain exceed thresholds between 5 and 20 people km⁻²; (ii) a moderate level of nature-based adaptation (NB 1), in which the population density threshold ranges between 20 and 150 people km⁻²; and (iii) a high level of nature-based adaptation (NB 2), with population density thresholds between 150 and 300 people km⁻². Changes in population growth during the simulation period are considered by applying a scenario of national population growth rates based on the Shared Socio-economic Pathway SSP2 (IIASA)²⁰, which is characterized by a moderate, and after 2070 slowing, global population growth, leading to 9 billion people by 2100²¹.

Under all SLR scenarios, 20 people km⁻² constitutes a crucial population density threshold. If a higher population density threshold is applied, more coastal wetlands have sufficient accommodation space to migrate inland resulting in an overall gain in global coastal wetland area (Fig. 1). If lower thresholds are considered, less coastal wetlands have sufficient accommodation space resulting in an overall global loss. The population density threshold of 20 people km⁻² corresponds to what we estimate as the current global average above which coastal communities are protected by some type of coastal protection infrastructure (Supplementary Information), hence allowing inland migration for only 37% of all global coastal wetlands. A population density threshold of 300 people km⁻² is the lower threshold for urban developments, as defined by the European Commission²², and sets the upper limit for potential wetland inland migration (NB 2 scenario). The highest SLR scenario at this threshold results in a substantial increase in global coastal wetland area (+60%). The same SLR scenario with a threshold population density of 5 people km⁻² results in a net global loss of 30% (Fig. 1). When applying the lowest SLR scenario, areal coastal wetland changes for population density thresholds between 5 and 300 people km⁻² only range between -8% (loss) and +15% (gain) (Fig. 1). The largest changes are observed for mangroves, which make the largest contribution to the global wetland area from the beginning (69%). Notably, much smaller losses are observed for salt marshes, even under the human adaptation scenarios with the least accommodation space (Fig. 1).

Under the BAU scenario for accommodation space (5–20 people km⁻²), changes in the extent of global coastal wetlands range between -8% (loss) and 0% (no change) for the lowest SLR scenario

and wetland inland migration is limited to where the population density in the 1-in-100-year floodplain falls below the respective threshold. Areal changes of all three wetland types (salt marsh, freshwater marsh and mangrove) are indicated in the tables below the graphs.

and between -30% (loss) and -8% (loss) for the highest SLR scenario. These losses can primarily be attributed to an increasing sediment deficiency, impeding the ability of the wetland to keep pace vertically with SLR. If, coastal wetlands are given more accommodation space in the future (for example, in the context of the implementation of nature-based adaptation solutions), global coastal wetlands could increase in areal extent (Fig. 1). Our moderate nature-based adaptation scenario (NB 1: 20–150 people km⁻²) results in an increase between 0% and 12% for the low, and between -8% (loss) and 42% for the high, SLR scenario. Under the more extreme adaptation scenario (NB 2: 150–300 people km⁻²), we anticipate even higher increases, between 12% and 15% for the low, and between 42% and 60% for the high, SLR scenario (Fig. 1). In contrast to the BAU scenario, these gains for the moderate and extreme nature-based adaptation scenarios (NB 1 and NB 2) are driven by inland wetland migration rather than vertical sediment accretion, and therefore independent of sediment availability.

Under the BAU scenario (lower boundary: 5 people km⁻²), most of the absolute loss in coastal wetland areas (approximately 66%) is projected to occur in the Caribbean Sea, the southern US east coast and parts of southeast Asia (Fig. 2a). Similarly, southeast Asia was previously identified¹⁹ as a highly critical region for mangrove resilience to SLR. The patterns of expected relative changes in wetland areas (that is, the percentage gain or loss) are different, but essentially confirm the Dynamic Interactive Vulnerability Assessment (DIVA) modelling results²; the largest relative area losses (again, under a scenario of highly constrained accommodation space) are found in the Caribbean Sea, along the eastern US coast and in the western Baltic Sea, the Mediterranean Sea, the Red Sea and parts of southeast Asia (Fig. 2b).

The spatial patterns of coastal wetland loss strongly resemble those of the modelled present-day sediment balance, namely the difference between the sediment required for a coastal wetland surface to keep pace vertically with current local relative SLR and the current-day sediment availability (Fig. 3). For example, large regions of sediment deficit are identified in the Caribbean Sea, western Baltic Sea, Mediterranean Sea, and along the eastern and western US coasts (Fig. 3). These areas largely coincide with the hotspot regions for relative wetland area losses under a scenario of highly constrained accommodation space (Fig. 2b). Meanwhile, most parts of Asia, South America and northwest Europe show sufficient or excess sediment availability (Fig. 3), which correspond to areas with small relative wetland loss, even where accommodation space is limited, as vertical sediment accretion counteracts relative SLR (Fig. 2b).

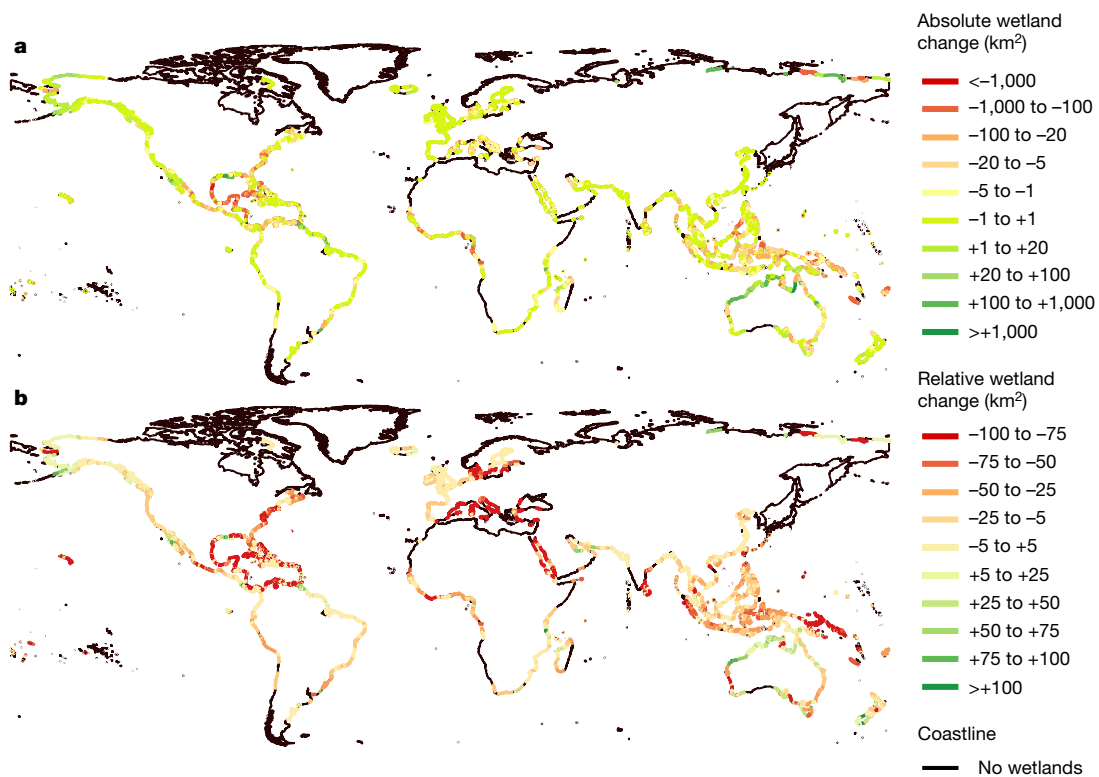


Fig. 2 | Spatial distribution of coastal wetland change. a, b, Absolute (a) and relative (b) changes in coastal wetland areas are displayed for the medium SLR scenario (RCP 4.5), assuming inhibition of wetland inland migration everywhere, but in (nearly) uninhabited regions with

a population density of less than 5 people km⁻². Population density is subject the population growth throughout the simulation period, following SSP2^{20,21}. The displayed coastline was generated during the DINAS-COAST FP5-EESD EU project (EVK2-CT-2000-00084).

Our sensitivity analysis confirms the importance of accounting for vertical sediment accretion with our ‘sediment accretion only’ scenario (hypothetical scenario (HYS) 2, Extended Data Table 2). This scenario reduces the global loss of coastal wetlands from 38% to 20%, 50% to 26% and 77% to 54% for the low, medium and high SLR scenarios, respectively, as compared to our ‘no resilience’ scenario, in which no accommodation space and no vertical sediment accretion are assumed (HYS 4; Extended Data Table 2, Extended Data Fig. 2).

Previous studies have highlighted the dangers of low sediment availability and reduced sediment supply, which may be exacerbated regionally by increasing the numbers of dams being built within river catchments, causing increased risk for coastal wetland loss with

SLR^{23–25}. However, our model sensitivity analysis under the high SLR scenario (RCP 8.5), and accounting for vertical sediment accretion, demonstrates that if present-day values of sediment supply were to change by ±50%, only a ±6% change in global wetland area would result (Extended Data Table 3). By contrast, accommodation space for inland wetland migration has a much stronger control on wetland persistence with SLR, yet much less is known about the actual process and further research is urgently needed. Our sensitivity analysis shows that even in heavily sediment-starved regions, an increase in accommodation space could result in a net wetland gain (Extended Data Fig. 3), particularly under high rates of SLR, even though the seaward side of the wetland could regularly be lost owing to the lack of sediment. Under

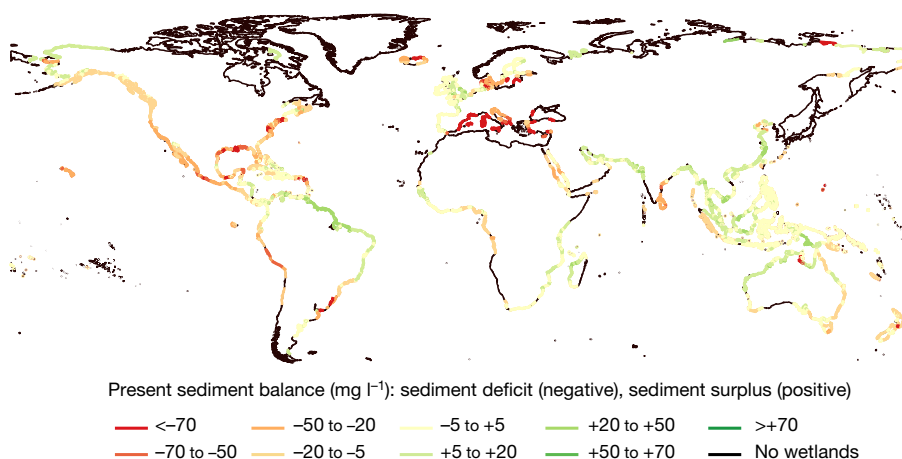


Fig. 3 | Present-day global sediment balance. Sediment surplus (positive values) or sediment deficit (negative values) (in mg l⁻¹) represent the difference between the suspended sediment concentration needed for coastal wetlands to build up vertically with current SLR rates and the

actual total suspended matter concentration derived from the satellite-borne GlobColour data (<http://globcolour.info>). The displayed coastline was generated during the DINAS-COAST FP5-EESD EU project (EVK2-CT-2000-00084).

extreme rates of SLR, and where sediment availability is insufficient, future coastal wetlands may therefore have a shorter lifetime and a lower degree of geomorphological, hydrological and biogeochemical complexity²⁶.

It should be noted that locally and especially in delta regions, these global mechanisms may not be as straightforward because historical and contemporary catchment and delta practices (for example, river damming and dredging) are responsible for much of the observed coastal wetland trends in many 'loss hotspots' rather than global SLR²⁷. Also, constraints on the inland migration of coastal wetlands may arise from adverse soil conditions, particularly where the inundated land has been intensively modified by humans, unsuitable geomorphological characteristics or elevation constraints (if located too low in the tidal frame)^{26,28}. To alleviate these constraints, coastal management strategies and engineering may locally be required to facilitate coastal wetlands to migrate inland²⁶. As a consequence, local patterns of wetland resilience may be at considerable variance with global estimates of change.

Our model projections suggest that nature-based adaptation solutions that maximize the inland migration of tidal wetlands in response to SLR, wherever possible, may help safeguard wetland persistence with SLR and protect associated ecosystem services. Existing nature-based adaptation solutions that allow coastal wetlands to migrate inland include the inland displacement of coastal flood defences (typically along highly engineered coastlines)¹² or the designation of nature reserve buffers in upland areas surrounding coastal wetlands¹⁸. These schemes, however, are currently implemented as local-scale projects only; strategically upscaling such projects, for example, as suggested by the shoreline management plans in England and Wales²⁹ or the coastal master plan in Louisiana³⁰, may help coastal wetlands adapt to SLR at the landscape scale and protect rapidly increasing global coastal populations.

Online content

Any methods, additional references, Nature Research reporting summaries, source data, statements of data availability and associated accession codes are available at <https://doi.org/10.1038/s41586-018-0476-5>

Received: 2 September 2017; Accepted: 25 July 2018;

Published online 12 September 2018.

- Blankespoor, B., Dasgupta, S. & Laplante, B. Sea-level rise and coastal wetlands. *Ambio* **43**, 996–1005 (2014).
- Spencer, T. et al. Global coastal wetland change under sea-level rise and related stresses: the DIVA Wetland Change Model. *Global Planet. Change* **139**, 15–30 (2016).
- Crosby, S. C. et al. Salt marsh persistence is threatened by predicted sea-level rise. *Estuar. Coast. Shelf Sci.* **181**, 93–99 (2016).
- Kirwan, M. L., Temmerman, S., Skeehean, E. E., Guntenspergen, G. R. & Fagherazzi, S. Overestimation of marsh vulnerability to sea level rise. *Nat. Clim. Chang.* **6**, 253–260 (2016).
- Schuerch, M., Vafeidis, A., Slawig, T. & Temmerman, S. Modeling the influence of changing storm patterns on the ability of a salt marsh to keep pace with sea level rise. *J. Geophys. Res. Earth Surf.* **118**, 84–96 (2013).
- French, J. R. Numerical simulation of vertical marsh growth and adjustment to accelerated sea-level rise, North Norfolk, U.K. *Earth Surf. Process. Landf.* **18**, 63–81 (1993).
- Morris, J. T., Sundareshwar, P. V., Nietch, C. T., Kjerfve, B. & Cahoon, D. R. Responses of coastal wetlands to rising sea level. *Ecology* **83**, 2869–2877 (2002).
- Enwright, N. M., Griffith, K. T. & Osland, M. J. Barriers to and opportunities for landward migration of coastal wetlands with sea-level rise. *Front. Ecol. Environ.* **14**, 307–316 (2016).
- Costanza, R. et al. Changes in the global value of ecosystem services. *Glob. Environ. Change* **26**, 152–158 (2014).
- Duarte, C. M., Losada, I. J., Hendriks, I. E., Mazarrasa, I. & Marba, N. The role of coastal plant communities for climate change mitigation and adaptation. *Nat. Clim. Chang.* **3**, 961–968 (2013).
- McLeod, E. et al. A blueprint for blue carbon: toward an improved understanding of the role of vegetated coastal habitats in sequestering CO₂. *Front. Ecol. Environ.* **9**, 552–560 (2011).

- Temmerman, S. et al. Ecosystem-based coastal defence in the face of global change. *Nature* **504**, 79–83 (2013).
- Möller, I. et al. Wave attenuation over coastal salt marshes under storm surge conditions. *Nat. Geosci.* **7**, 727–731 (2014).
- Shepard, C. C., Crain, C. M. & Beck, M. W. The protective role of coastal marshes: a systematic review and meta-analysis. *PLoS One* **6**, e27374 (2011).
- Stark, J., Van Oyen, T., Meire, P. & Temmerman, S. Observations of tidal and storm surge attenuation in a large tidal marsh. *Limnol. Oceanogr.* **60**, 1371–1381 (2015).
- Aburto-Oropeza, O. et al. Mangroves in the Gulf of California increase fishery yields. *Proc. Natl Acad. Sci. USA* **105**, 10456–10459 (2008).
- Teuchies, J. et al. Estuaries as filters: the role of tidal marshes in trace metal removal. *PLoS One* **8**, e70381 (2013).
- Kirwan, M. L. & Megonigal, J. P. Tidal wetland stability in the face of human impacts and sea-level rise. *Nature* **504**, 53–60 (2013).
- Lovelock, C. E. et al. The vulnerability of Indo-Pacific mangrove forests to sea level rise. *Nature* **526**, 559–563 (2015).
- van Vuuren, D. P. et al. A new scenario framework for climate change research: scenario matrix architecture. *Clim. Change* **122**, 373–386 (2014).
- Kc, S. & Lutz, W. The human core of the shared socioeconomic pathways: population scenarios by age, sex and level of education for all countries to 2100. *Glob. Environ. Change* **42**, 181–192 (2017).
- Dijkstra, L. & Poelman, H. *A Harmonised Definition of Cities and Rural Areas: the New Degree of Urbanisation*; European Commission Working Paper WP 01/2014 (2014).
- Day, J. W., Pont, D., Hensel, P. F. & Ibáñez, C. Impacts of sea-level rise on deltas in the Gulf of Mexico and the Mediterranean: the importance of pulsing events to sustainability. *Estuaries* **18**, 636–647 (1995).
- Yang, S. L. et al. Impact of dams on Yangtze River sediment supply to the sea and delta intertidal wetland response. *J. Geophys. Res. Earth Surf.* **110**, F03006 (2005).
- Ganju, N. K. et al. Spatially integrative metrics reveal hidden vulnerability of microtidal salt marshes. *Nat. Commun.* **8**, 14156 (2017).
- Spencer, K. L. et al. Physicochemical changes in sediments at Orplands Farm, Essex, UK following 8 years of managed realignment. *Estuar. Coast. Shelf Sci.* **76**, 608–619 (2008).
- Jankowski, K., Törnqvist, T. E. & Fernandes, A. M. Vulnerability of Louisiana's coastal wetlands to present-day rates of relative sea-level rise. *Nat. Commun.* **8**, 14792 (2017).
- French, P. W. Managed realignment — the developing story of a comparatively new approach to soft engineering. *Estuar. Coast. Shelf Sci.* **67**, 409–423 (2006).
- Nicholls, R. J., Townend, I. H., Bradbury, A. P., Ramsbottom, D. & Day, S. A. Planning for long-term coastal change: experiences from England and Wales. *Ocean Eng.* **71**, 3–16 (2013).
- Peyronnin, N. et al. Louisiana's 2012 coastal master plan: overview of a science-based and publicly informed decision-making process. *J. Coast. Res.* **67**, 1–15 (2013).

Acknowledgements This research was financially supported by the Deutsche Forschungsgemeinschaft (DFG) through the Cluster of Excellence 80 'The Future Ocean', funded within the framework of the Excellence Initiative on behalf of the German federal and state governments, the personal research fellowship of M.S. (project number 272052902) and by the Cambridge Coastal Research Unit (Visiting Scholar Programme). Furthermore, this work has partly been supported by the European Union's Seventh Programme for Research, Technological Development and Demonstration (grant no. 603396, RISE-AM project), the European Union's Horizon 2020 Research and Innovation Programme (grant no. 642018, GREEN-WIN project), the US National Science Foundation (Coastal SEES 1426981 and NSF CAREER 1654374), Deltares and the UK Natural Environment Research Council. We thank M. Martin for support in editing the calibration data and G. Amable for statistical advice.

Reviewer information Nature thanks B. Glavovic, J. Woodruff and the other anonymous reviewer(s) for their contribution to the peer review of this work.

Author contributions M.S. and T.S. developed the model algorithm. M.S. and D.L. developed the model code. M.S., C.W., C.McC., M.D.P., M.L.K., A.T.V., R.R. and S.B. gathered and produced input data. M.S., S.T. and R.J.N. analysed and interpreted the model simulations. M.S., T.S., S.T., M.L.K. and J.H. wrote the paper.

Competing interests The authors declare no competing interests.

Additional information

Extended data is available for this paper at <https://doi.org/10.1038/s41586-018-0476-5>.

Supplementary information is available for this paper at <https://doi.org/10.1038/s41586-018-0476-5>.

Reprints and permissions information is available at <http://www.nature.com/reprints>.

Correspondence and requests for materials should be addressed to M.S. **Publisher's note:** Springer Nature remains neutral with regard to jurisdictional claims in published maps and institutional affiliations.

METHODS

General description of model approach. Our model is based on the construction of coastal profiles for 12,148 coastline segments. These segments constitute the spatial units of the Dynamic Interactive Vulnerability Assessment (DIVA) modelling framework^{31,32}. The coastal profiles are derived from the Shuttle Radar Topography Mission (SRTM) floodplain data, available from the global DIVA database³³. Within each coastline segment, the existing coastal wetlands, as reported by the United Nations Environment Programme World Conservation Monitoring Centre (UNEP WCMC)^{34,35}, are assumed to be located between mean sea level (MSL) and mean high water spring (MHWS) level. With SLR, the seaward side of the wetlands are increasingly inundated ('unconstrained wetland loss'), while the landward side migrates inland by converting terrestrial uplands to coastal wetlands³⁶ (Extended Data Fig. 5). However, inland wetland migration may be inhibited by anthropogenic coastal infrastructure that reduces the available accommodation space^{36–39}, a variable that we approximate with the population density in the floodplain of the 1-in-100-year extreme water level (Extended Data Fig. 4).

Seaward wetland loss through inundation is counteracted by a large tidal range and a high sediment availability, as both these variables increase the resilience of coastal wetlands towards drowning through vertical sediment accretion processes^{19,40–44}. This is represented by the wetland adaptability score (WAS) reducing the loss of wetlands where tidal range and sediment availability are high⁴⁰ (Extended Data Fig. 4). The calculation of the WAS is based on a linear relationship between sediment availability and wetland drowning, whereas the slope of the linear relationship depends on tidal range. This relationship was suggested previously⁴⁰, when an ensemble of five different tidal marsh accretion models was used to identify the critical rates of relative SLR as a function of tidal range and sediment availability.

Following the calculation of the seaward wetland loss and inland wetland gain, the resulting global coastal wetland areas are calculated for every model time step (5 years) between 2010 and 2100. The model is driven by temporal changes in the model variables 'regional relative sea level rise' and 'population density' according to a range of regionalized scenarios for global SLR (RCPs)⁴⁵ and SSP2²⁰ for national population growth, respectively (Extended Data Table 2, Extended Data Fig. 4).

Database and data model. The input variables are derived from spatially explicit global data sets. They are attributed to the 12,148 coastline segments³¹, which have an average length of 57 km. Coastline segmentation is a product of the DIVA modelling framework; the related database includes more than 100 bio-physical and socio-economic parameters³¹. The dissection of the global coastline into segments is based on the concept described previously⁴⁶, where coastal units have been created such that bio-physical and socio-economic impacts of global SLR are expected to be comparable within each coastline segment.

Construction of the coastal topographic profile. For each of the DIVA coastline segments, the coastal topographical profile is approximated using the areal information on coastal floodplains as described previously³². Floodplain areas (km²) are provided for the elevation increments <1.5 m, 1.5–2.5 m, 2.5–3.5 m, 3.5–4.5 m, 4.5–5.5 m, 5.5–8.5 m, 8.5–12.5 m and 12.5–16.5 m, based on freely available SRTM data⁴⁷. The SRTM data have a 90 m horizontal and a 1 m vertical resolution. The coastal profiles are constructed by dividing the floodplain areas per elevation increment by the length of the corresponding coastline segment to calculate the inundation lengths, which are then plotted against the upper boundaries of the elevation increments (that is, 1.5 m, 2.5 m, 3.5 m and so on) (Extended Data Fig. 5). It is thereby assumed that elevations continuously increase with distance from the coast, which has been shown to be a reasonable assumption³³.

Elevations between the upper boundaries of the elevation increments are linearly interpolated following earlier global assessments^{32,48–50}. Linear interpolation between the MHWS level and an elevation of 1.5 m (or higher) was previously shown^{51,52} to approximate high resolution LIDAR-derived elevations with a mean error of less than 30 cm and to produce no systematic bias with respect to the area of inundated land, even for the lowest 50 cm of the profile⁵².

Wetland data. The areal wetland extents used in the context of this study include current wetland areas (1973–2015) for mangrove forests³⁴, salt marshes³⁵ and tidal freshwater marshes⁵³. On the basis of a literature search for the lower and upper elevation limits of mangroves, salt marshes and tidal freshwater marshes^{54–58}, we assume that all coastal wetland types are located at elevations between MSL and MHWS and can occur over the entire elevation range. The reported wetland areas for each coastline segment are distributed alongside the non-wetland floodplain on the previously constructed coastal profile (Extended Data Fig. 5). We appreciate that in nature, the upper and lower boundaries of coastal wetlands will vary as a result of different vegetation species, tidal currents and waves⁵⁹, but for our global application MSL as the lower, and MHWS as the upper, limit constitute solid boundaries.

Regional relative sea-level rise data and scenarios. We use three SLR scenarios, covering the range of global SLR as projected by the IPCC AR5⁴⁵ plus a possible greater contribution of ice-sheets as assessed on the basis of post-AR5 methods³².

The three scenarios represent the RCPs 2.6, 4.5 and 8.5, paired with a low, medium and high ice-sheet contribution, respectively, and generated using the general circulation model HadGEM2-ES⁶⁰ (Extended Data Table 2). The SLR scenarios are regionalized, therefore accounting for regional gravitational and rotational effects due to changes in ice mass distribution and steric variation³². Local relative SLR information is attained by combining the regionalized SLR projections with segment-specific vertical land movement based on a global model of glacial isostatic adjustment⁶¹ and some additional 2 mm yr⁻¹ of natural subsidence in large river deltas^{62,63} (Extended Data Fig. 6). Meanwhile, human-induced subsidence, which may be of particular importance in large river deltas⁶⁴, is not considered for calculating regional relative SLR. However, a sensitivity analysis using delta-wide subsidence rates of 5 mm yr⁻¹ showed only small deviation in modelled overall global wetland areas (Extended Data Table 4). Tectonic and neotectonic uplift and subsidence processes, other than glacial isostatic adjustment, are also not included owing to the lack of an appropriate global data set.

Tidal range data. To calculate the WAS (Extended Data Fig. 4) and compute the vertical wetland extent within each coastline segment, we use a newly developed global tidal range data set⁶⁵, representing the segment-specific tidal range (that is, the difference between mean low water and mean high water), mean high water neap (MHWN) and mean high water spring (MHWS) tidal levels. The new tidal dataset was generated using OTISmp⁶⁶, a forward global tidal model, solving the nonlinear shallow water equations on a C-grid using a finite differences time stepping method (Supplementary Information).

Population density data. For each coastline segment, the coastal population within each elevation increment is computed by superimposing the SRTM digital elevation model⁴⁷ with the Global Rural-Urban Mapping Project (GRUMP) population data⁶⁷, being subject to national population growth according to SSP2 (IIASA)^{20,68}. To determine the population density in the floodplain of the 1-in-100-year extreme water level, which is used as a proxy for the availability of accommodation space (Extended Data Fig. 4), we derive the hydrologically connected floodplain area for the 1-in-100-year extreme water level and the corresponding population affected by flooding³². We use the latest dataset on extreme water levels along the world's coastline, produced with a new global storm surge model hindcasting extreme water levels between 1979 and 2014³⁰. Extreme water levels are reported for the return periods of 1, 10, 100 and 1,000 years and are derived from total water levels during storm surge events, thus including both tides and surges.

Sediment availability data. Local sediment availability is derived from MERIS satellite data, processed in the framework of the GlobColour project (<http://globcolour.info>). The data represent total suspended matter in the water column and have been developed, validated, and distributed by ACRI-ST, France⁶⁹. We use the monthly averages from April 2002 to April 2012 that have a horizontal resolution of 1/24°. A long-term average is calculated for every pixel, and an average value of all pixels located within a 4 km buffer of each coastline segment is used to represent the local sediment availability (mg l⁻¹).

Conversion of terrestrial upland to coastal wetlands. With increasing sea levels, we allow coastal wetlands to migrate inland, a process that we understand as the establishment of wetland vegetation inland of its previous location, by raising the MHWS level along the coastal profile. Hence, former terrestrial upland areas are inundated and converted to coastal wetlands (Extended Data Fig. 5), based on elevation, where no human barriers are assumed to be present^{36–39}. This modelling approach is supported by recent local-scale field studies for coastal salt marshes at the US east coast and in the Gulf of Mexico^{70–74} and has previously been applied through various local-scale models, both for salt marshes and mangroves^{75–79}. The establishment of coastal wetland vegetation in inundated upland areas is assumed to be associated with a response lag of five years, which is in line with evidence produced by recent wetland restoration studies^{80–83}. However, the development of related wetland functions (such as biogeochemical functioning) may take longer^{74,80}.

For calculation of the converted upland areas, we assume the segment-specific wetland/non-wetland proportion to remain constant over time, whereby the non-wetland area within a coastline segment equals the total floodplain area (that is, the total interpolated area between MSL and MHWS) minus the reported wetland area. The conversion of uplands to wetlands is therefore calculated as the product of the wetland/non-wetland proportion and the total inundated upland area. However, conversion of terrestrial upland to coastal wetland is assumed to be zero where the coastal population density within the floodplain of the 1-in-100-year extreme water level exceeds the given thresholds (5, 20, 150 or 300 people km⁻²), representing the existence of anthropogenic barriers to inland wetland migration. We thereby assume that coastal protection infrastructure is an important contributor to anthropogenic barriers for wetland inland migration^{2,8,36–39} and is built where coastal communities are threatened by extreme water levels, such as a 1-in-100-year event^{32,84}.

Seaward loss of coastal wetlands. As sea level rises, not only the upper wetland boundary (MHWS) but also the lower wetland boundary (MSL) shifts position,

potentially causing inundation of coastal wetlands beyond physiological tolerance. Therefore, we calculate an ‘unconstrained seaward loss’ that at first neglects the capacity of the wetland to adapt vertically to SLR by sediment accretion. Through sediment accretion, this unconstrained seaward loss may, however, be reduced or inhibited, given sufficient sediment availability within the coastline segment (Extended Data Fig. 4).

The WAS is a measure for the difference between the sediment needed for the coastal wetland to vertically accrete sediment as fast as SLR and the sediment available. It represents a sediment surplus if positive, and a sediment deficit if negative (Fig. 3). The amount of sediment needed for a coastal wetland to adapt to SLR has been studied previously⁴⁰, using an ensemble of five models for tidal marsh accretion. Linear relationships were presented between sediment availability and the maximum rate of relative SLR that a tidal marsh can survive, showing steeper slopes (higher resilience) for marshes in macrotidal environments compared to marshes in microtidal environments⁴⁰. We directly use these linear relationships for our tidal marshes (including tidal salt and freshwater marshes), whereas we modify the model parameters for modelling mangrove forests during our calibration procedure (Supplementary Information). The local sediment availability, as derived from the GlobColour data, is assumed to represent the current levels of total suspended matter in the coastal zone and assumed to remain constant during the simulation period. To account for possible changes in future global sediment supply, a sensitivity analysis has been conducted with average sediment availability levels reduced and increased by 20% and 50% (Extended Data Table 3).

The WAS thus represents the ability of the coastal wetlands within a coastline segment to adapt to rising sea levels by sediment accretion. A positive WAS value indicates that sediment availability is sufficient to maintain the present wetland area, whereas a negative WAS value suggests that coastal wetlands are inundated and (partially) lost in response to SLR. The WAS is an integer value that ranges from -5 to $+5$, indicating a very high (-5) to very low (-1) sediment deficiency and a very low ($+1$) to very high ($+5$) sediment surplus, respectively. On the basis of the WAS, the unconstrained seaward loss (SL_{unc} ; km^2) is transformed into a constrained seaward loss (SL_c ; km^2), assuming a linear relationship between WAS and the proportion of inundated wetland actually being lost, but only if WAS is negative (equation (1)). No wetland loss is computed where WAS is positive or zero. With SLR, both the WAS and SL_{unc} change over time. Thus, SL_c is updated after every time step (t_i).

$$SL_c(t_i) = (-1/5) \times WAS(t_i) \times SL_{unc}(t_i) \quad (1)$$

The calculation of WAS is based on the assumption that the critical rate of relative SLR ($RSLR_{crit}$; $mm\ yr^{-1}$) depends on sediment availability (Sed; $mg\ l^{-1}$) and tidal range (TR), as suggested previously⁴⁰. The previous modelling results⁴⁰ can be approximated using the following relationship (equation (2)):

$$RSLR_{crit} = (m \times TR^e) \times Sed + i \quad (2)$$

in which $(m \times TR^e)$ represents the slope of a linear relationship between $RSLR_{crit}$ and Sed. Model parameters e , i and m are calibrated separately for tidal marshes (including tidal salt and freshwater marshes, e_{TF} , i_{TF} and m_{TF}) and mangrove systems (e_{Man} , i_{Man} and m_{Man}). Parameters e_{TF} , i_{TF} and m_{TF} are directly derived from the model ensemble runs described previously⁴⁰, and e_{Man} , i_{Man} and m_{Man} are estimated by calibrating the model using the mangrove data presented previously¹⁹ (Supplementary Information).

To estimate the sediment needed for a given SLR rate, Sed_{crit} ($mg\ l^{-1}$), we rewrite equation (2) as follows (equation (3)):

$$Sed_{crit} = (RSLR - i) / (m \times TR^e) \quad (3)$$

in which $RSLR$ ($mm\ yr^{-1}$) is the actual (time-dependent) local relative SLR rate. Knowing the current sediment availability (Sed) within each coastline segment (derived from the GlobColour data), we compare this value with the segment-specific Sed_{crit} and define WAS as the scaled and rounded difference between the available and needed sediment availability (equation (4)):

$$WAS = \text{round}\{[(Sed - Sed_{crit})/a] \times 5\} \quad (4)$$

in which a represents the sediment surplus (or deficit in case $Sed_{sup} < Sed_{sup,crit}$), which is considered as ‘very high’. The determination of a is subject to model calibration (Supplementary Information). All WAS values greater (smaller) than 5 (-5) are transformed to WAS values of 5 (-5).

Model calibration. The model parameters m_{TF} , m_{Man} , e_{TF} , e_{Man} , i_{TF} , i_{Man} and a (equations (3) and (4)) are estimated using a stepwise calibration procedure as described in detail in the Supplementary Information. Model results are thereby compared to field measurements of vertical elevation growth for 39 marsh sites across US and European Atlantic shorelines⁴, 18 marsh sites in North America, Europe and northeast Australia³ and 26 mangrove sites across Pacific shorelines¹⁹.

The calibrated model ($m_{TF} = 3.42$, $m_{Man} = 4.42$, $e_{TF} = 0.915$, $e_{Man} = 1.18$, $i_{TF} = -1.5$, $i_{Man} = 0$ and $a = 40\ mg\ l^{-1}$) correctly predicts whether there is a sediment deficit, a sediment surplus or a balanced sediment budget for 78% of the coastline segments where field data are available (Extended Data Table 1).

Scenarios. The three SLR scenarios RCP 2.6, 4.5 and 8.5, accounting for the full range of available SLR scenarios⁴⁵, are combined with three human adaption scenarios. These are subject to population growth according to SSP2 (Extended Data Table 2), which is considered a middle-of-the-road scenario for population growth⁶⁸. The three different human adaptation scenarios include a BAU scenario, and a moderate (NB 1) and an extreme (NB 2) nature-based adaptation scenario. They reflect differences in the potential of coastal wetlands to migrate inland until 2100 owing to potential differences in future coastal management strategies. In addition, four different physically and/or socio-economically unrealistic model configurations (Extended Data Table 2: hypothetical scenarios) are used during the sensitivity analysis to quantify the extent to which overall resilience is enabled/constrained by vertical and horizontal adaptability mechanisms, namely vertical sediment accretion and wetland inland migration.

Human adaptation scenarios. Inland/upward migration of coastal wetlands is often obstructed by the presence of anthropogenic infrastructure (for example, dikes, seawalls, cities, roads and railways)^{18,37}. As there is no global dataset on coastal infrastructure, we approximate accommodation space through a population density threshold above which we assume that no accommodation space is available for coastal wetlands to migrate inland/upward. We thereby assume that coastal infrastructure is more likely to be present where population density is high^{37,85}, and that coastal protection structures are among the most important barriers for wetland inland migration⁸. By comparing a recent expert judgement on current coastal protection infrastructure, relying on population density and gross national income⁸⁶, with coastal population densities within the 1-in-100-year extreme water level floodplain, we find that currently, on a global average, coasts of $>20\ people\ km^{-2}$ are protected by some kind of coastal protection infrastructure (Supplementary Information). We consider this number as the upper boundary of current accommodation space. This is because it only includes coastal protection infrastructure and neglects other anthropogenic infrastructure that may act as barrier. As a lower boundary we choose a population density threshold of $5\ people\ km^{-2}$ as this has previously been used to define (nearly) uninhabited land⁸⁷. We therefore define the range of threshold population densities between 5 and $20\ people\ km^{-2}$ as our BAU scenario (Fig. 1 and Extended Data Table 2).

In two nature-based adaptation scenarios (NB 1 and NB 2), we assume that coastal societies in rural areas retreat from the coast with SLR, removing coastal protection and other infrastructure that inhibit inland migration of coastal wetlands. We thereby assume that this is more likely to happen in sparsely populated areas as compared to densely populated areas^{8,88–90}. For the first NB 1 scenario, we assume an upper boundary of $150\ people\ km^{-2}$, which corresponds to the Organisation for Economic Co-operation and Development (OECD) definition of urban areas⁹¹. In the second, more extreme NB 2 scenario, we use a threshold of $300\ people\ km^{-2}$ as the upper boundary, as this corresponds to the European Commission’s definition of urban areas²² (Extended Data Table 2).

Hypothetical scenarios. The four hypothetical scenarios used for the sensitivity analysis include: (1) wetland migration only, characterized by the exclusion of bio-physical vertical accretion mechanisms and unlimited inland accommodation space; (2) sediment accretion only, characterized by the inclusion of bio-physical vertical accretion mechanisms, but assuming no inland accommodation space; (3) maximum resilience, which includes bio-physical accretion mechanisms and assumes an unlimited potential for inland migration; and (4) no resilience, in which neither bio-physical accretion nor inland migration are accounted for (Extended Data Table 2).

It should be noted that these hypothetical scenarios are unrealistic from a socio-economic or physical perspective, because no future coast will be neither completely defended nor completely undefended by dikes and seawalls and neither will sediment accretion be fully absent. But these hypothetical model runs are meant to demonstrate the relative contributions of the two mechanisms of wetland inland migration and sediment accretion to the overall wetland resilience to SLR.

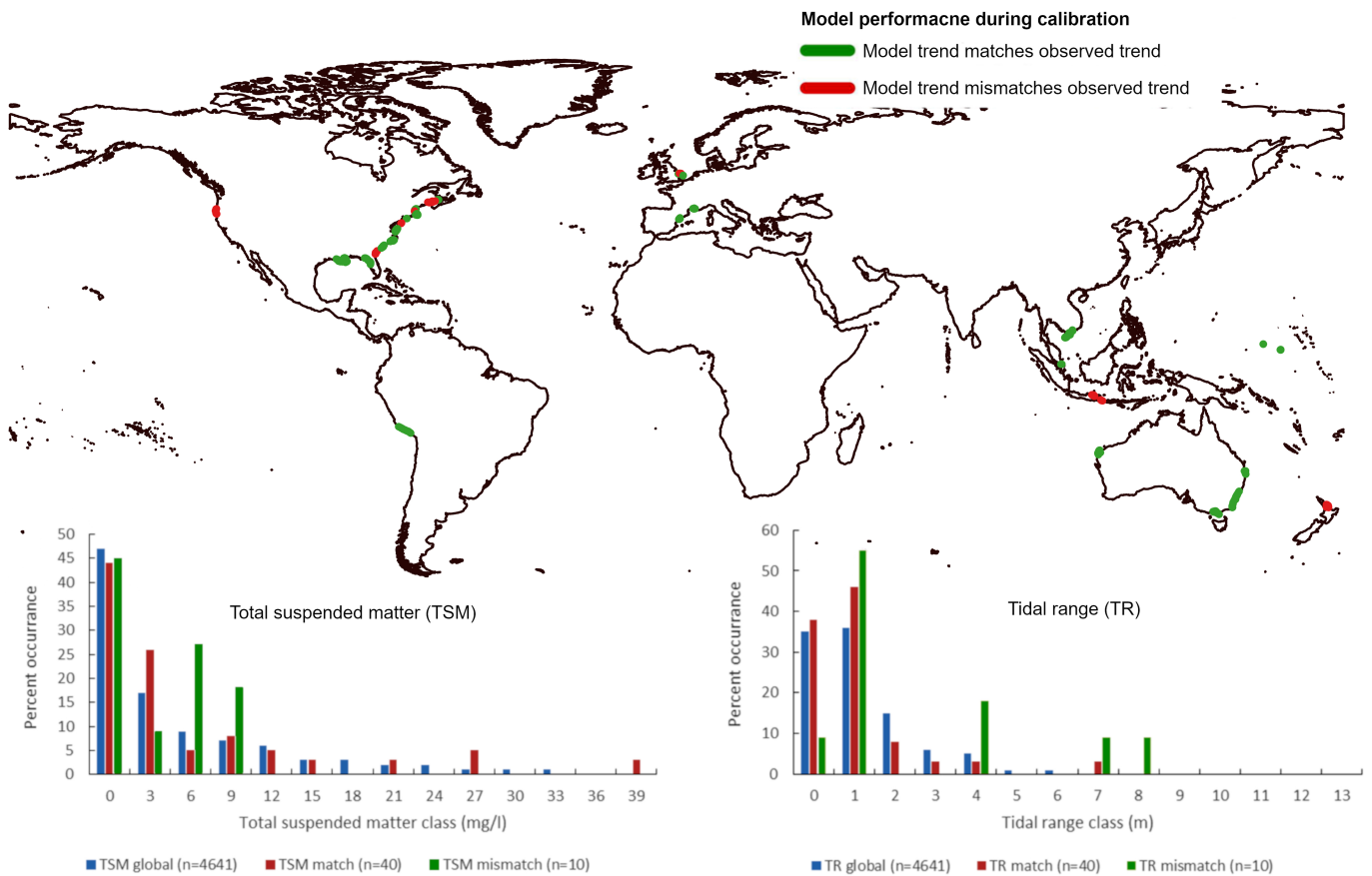
Reporting summary. Further information on research design is available in the Nature Research Reporting Summary linked to this paper.

Code availability. The computer code that supports the findings of this study is available for non-commercial use (CC BY-NC-SA 4.0) from the GitLab repository ‘global-coastal-wetland-model’, <https://gitlab.com/mark.schuerch/global-coastal-wetland-model.git>. Registration on GitLab is required to access the repository.

Data availability. The data that support the findings of this study are available from the corresponding author upon reasonable request. The Source Data for Fig. 1 and Extended Data Fig. 2 are provided.

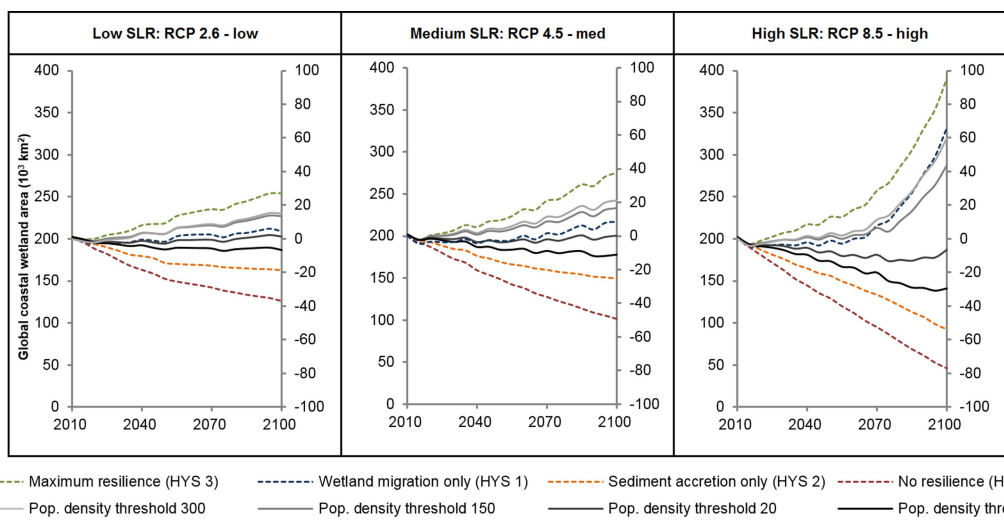
31. Vafeidis, A. T. et al. A new global coastal database for impact and vulnerability analysis to sea-level rise. *J. Coastal Res.* **24**, 917–924 (2008).

32. Hinkel, J. et al. Coastal flood damage and adaptation costs under 21st century sea-level rise. *Proc. Natl Acad. Sci. USA* **111**, 3292–3297 (2014).
33. Vafeidis, A. T. et al. Water-level attenuation in broad-scale assessments of exposure to coastal flooding: a sensitivity analysis. *Natural Hazards and Earth System Sciences Discussions* <https://doi.org/10.5194/nhess-2017-199> (2017).
34. Giri, C. et al. Status and distribution of mangrove forests of the world using earth observation satellite data. *Glob. Ecol. Biogeogr.* **20**, 154–159 (2011).
35. McOwen, C. et al. A global map of saltmarshes. *Biodivers. Data J.* **5**, e11764 (2017).
36. Kirwan, M. L., Walters, D. C., Reay, W. G. & Carr, J. A. Sea level driven marsh expansion in a coupled model of marsh erosion and migration. *Geophys. Res. Lett.* **43**, 4366–4373 (2016).
37. Borchert, S. M., Osland, M. J., Enwright, N. M. & Griffith, K. T. Coastal wetland adaptation to sea level rise: quantifying potential for landward migration and coastal squeeze. *J. Appl. Ecol.* <https://doi.org/10.1111/1365-2664.13169> (2018).
38. Gilman, E. L., Ellison, J., Duke, N. C. & Field, C. Threats to mangroves from climate change and adaptation options: a review. *Aquat. Bot.* **89**, 237–250 (2008).
39. Torio, D. D. & Chmura, G. L. Assessing Coastal Squeeze of Tidal Wetlands. *J. Coast. Res.* **29**, 1049–1061 (2013).
40. Kirwan, M. L. et al. Limits on the adaptability of coastal marshes to rising sea level. *Geophys. Res. Lett.* **37**, L23401 (2010).
41. D'Alpaos, A., Mudd, S. M. & Carniello, L. Dynamic response of marshes to perturbations in suspended sediment concentrations and rates of relative sea level rise. *J. Geophys. Res. Earth Surf.* **116**, F04020 (2011).
42. French, J. Tidal marsh sedimentation and resilience to environmental change: exploratory modelling of tidal, sea-level and sediment supply forcing in predominantly allochthonous systems. *Mar. Geol.* **235**, 119–136 (2006).
43. Kirwan, M. L. & Guntenspergen, G. R. Influence of tidal range on the stability of coastal marshland. *J. Geophys. Res. Earth Surf.* **115**, F02009 (2010).
44. Temmerman, S., Govers, G., Wartel, S. & Meire, P. Modelling estuarine variations in tidal marsh sedimentation: response to changing sea level and suspended sediment concentrations. *Mar. Geol.* **212**, 1–19 (2004).
45. Church, J. A. et al. in *Climate Change 2013: the Physical Science Basis. Contribution of Working Group I to the Fifth Assessment Report of the Intergovernmental Panel on Climate Change* (eds Stocker, T. F. et al.) 1137–1216 (Cambridge Univ. Press, Cambridge, 2013).
46. McFadden, L., Nicholls, R. J., Vafeidis, A. & Tol, R. S. J. Methodology for modeling coastal space for global assessment. *J. Coast. Res.* **23**, 911–920 (2007).
47. Jarvis, A., Reuter, H. I., Nelson, A. & Guevara, E. *Hole-Filled SRTM for the Globe Version 4*; <http://srtm.csi.cgiar.org/> (2008).
48. Nicholls, R. J., Hoozemans, F. & Marchand, M. Increasing flood risk and wetland losses due to global sea-level rise: regional and global analyses. *Glob. Environ. Change* **9**, 69–87 (1999).
49. Nicholls, R. J. Coastal flooding and wetland loss in the 21st century: changes under the SRES climate and socio-economic scenarios. *Glob. Environ. Change* **14**, 69–86 (2004).
50. Muis, S., Verlaan, M., Winsemius, H. C., Aerts, J. C. J. H. & Ward, P. J. A global reanalysis of storm surges and extreme sea levels. *Nat. Commun.* **7**, 11969 (2016).
51. Titus, J. G. & Richman, C. Maps of lands vulnerable to sea level rise modeled elevations along the US Atlantic and Gulf coasts. *Clim. Res.* **18**, 205–228 (2001).
52. Titus, J. G. & Wang, J. in *Background Documents Supporting Climate Change Science Program Synthesis and Assessment Product 4.1 (EPA 430R07004)* (eds Titus, J. G. & Strange, E. M.) (United States Environmental Protection Agency (EPA), Washington DC, 2008).
53. Vafeidis, A. T., Nicholls, R. J., McFadden, L., Hinkel, J. & Grasshoff, P. S. Developing a global database for coastal vulnerability analysis: design issues and challenges. *Int. Arch. Photogramm. Remote Sens. Spat. Inf. Sci.* **35**, 801–805 (2004).
54. Balke, T., Stock, M., Jensen, K., Bouma, T. J. & Kleyer, M. A global analysis of the seaward salt marsh extent: the importance of tidal range. *Wat. Resour. Res.* **52**, 3775–3786 (2016).
55. Ellison, J. in *Coastal Wetlands: an Integrated Ecosystem Approach* (eds Perillo, G. M. E. et al.) 565–591 (Elsevier, Amsterdam, 2009).
56. McIvor, A. L., Spencer, T., Möller, I. & M., S. *The Response of Mangrove Soil Surface Elevation to Sea Level Rise* (The Nature Conservancy and Wetlands International, 2013).
57. McKee, K. L. & Patrick, W. H. The relationship of smooth cordgrass (*Spartina alterniflora*) to tidal datums: a review. *Estuaries* **11**, 143–151 (1988).
58. Odum, W. E. Comparative ecology of tidal freshwater and salt marshes. *Annu. Rev. Ecol. Syst.* **19**, 147–176 (1988).
59. Gray, A. J., Marshall, D. F. & Raybould, A. F. A century of evolution in *Spartina anglica*. *Adv. Ecol. Res.* **21**, 1–62 (1991).
60. Jones, C. D. et al. The HadGEM2-ES implementation of CMIP5 centennial simulations. *Geosci. Model Dev.* **4**, 543 (2011).
61. Peltier, W. Global glacial isostasy and the surface of the ice-age earth: the ice-5G (VM2) model and GRACE. *Annu. Rev. Earth Planet. Sci.* **32**, 111–149 (2004).
62. Meckel, T. A., Ten Brink, U. S. & Williams, S. J. Sediment compaction rates and subsidence in deltaic plains: numerical constraints and stratigraphic influences. *Basin Res.* **19**, 19–31 (2007).
63. Syvitski, J. P. M. Deltas at risk. *Sustain. Sci.* **3**, 23–32 (2008).
64. Ericson, J. P., Vörösmarty, C. J., Dingman, S. L., Ward, L. G. & Meybeck, M. Effective sea-level rise and deltas: causes of change and human dimension implications. *Global Planet. Change* **50**, 63–82 (2006).
65. Pickering, M. D. et al. The impact of future sea-level rise on the global tides. *Cont. Shelf Res.* **142**, 50–68 (2017).
66. Egbert, G. D., Ray, R. D. & Bills, B. G. Numerical modeling of the global semi-diurnal tide in the present day and in the last glacial maximum. *J. Geophys. Res. Oceans* **109**, C03003 (2004).
67. Center for International Earth Science Information Network (CIESIN) Columbia University, International Food Policy Research Institute (IFPRI), The World Bank & Centro Internacional de Agricultura Tropical (CIAT). *Global Rural-Urban Mapping Project, Version 1 (GRUMPv1): Population Density Grid*; <http://doi.org/10.7927/H4R2OZ93> (accessed 22 July 2016).
68. Fricko, O. et al. The marker quantification of the Shared Socioeconomic Pathway 2: a middle-of-the-road scenario for the 21st century. *Glob. Environ. Change* **42**, 251–267 (2017).
69. Barrot, G., Mangin, A. & Pinnock, S. *Global Ocean Colour for Carbon Cycle Research, Product User Guide* (ACRI-ST, Sophia-Antipolis, 2007).
70. Raabe, E. A. & Stumpf, R. P. Expansion of Tidal Marsh in Response to Sea-Level Rise: Gulf Coast of Florida, USA. *Estuaries Coasts* **39**, 145–157 (2016).
71. Schieder, N. W., Walters, D. C. & Kirwan, M. L. Massive upland to wetland conversion compensated for historical marsh loss in Chesapeake Bay, USA. *Estuaries Coasts* **41**, 940–951 (2018).
72. Smith, J. A. M. The role of *Phragmites australis* in mediating inland salt marsh migration in a mid-atlantic estuary. *PLoS One* **8**, e65091 (2013).
73. Langston, A. K., Kaplan, D. A. & Putz, F. E. A casualty of climate change? Loss of freshwater forest islands on Florida's Gulf Coast. *Glob. Change Biol.* **23**, 5383–5397 (2017).
74. Anisfeld, S. C., Cooper, K. R. & Kemp, A. C. Upslope development of a tidal marsh as a function of upland land use. *Glob. Change Biol.* **23**, 755–766 (2017).
75. Feagin, R. A., Martinez, M. L., Mendoza-Gonzalez, G. & Costanza, R. Salt marsh zonal migration and ecosystem service change in response to global sea level rise: a case study from an urban region. *Ecol. Soc.* **15**, 14 (2010).
76. Gilman, E., Ellison, J. & Coleman, R. Assessment of mangrove response to projected relative sea-level rise and recent historical reconstruction of shoreline position. *Environ. Monit. Assess.* **124**, 105–130 (2007).
77. Di Nitto, D. et al. Mangroves facing climate change: landward migration potential in response to projected scenarios of sea level rise. *Biogeosciences* **11**, 857–871 (2014).
78. Rogers, K., Saintilan, N. & Copeland, C. Managed retreat of saline coastal wetlands: challenges and opportunities identified from the Hunter River Estuary, Australia. *Estuaries Coasts* **37**, 67–78 (2014).
79. Stralberg, D. et al. Evaluating tidal marsh sustainability in the face of sea-level rise: a hybrid modeling approach applied to San Francisco Bay. *PLoS One* **6**, e27388 (2011).
80. Craft, C., Broome, S. & Campbell, C. Fifteen years of vegetation and soil development after brackish-water marsh creation. *Restor. Ecol.* **10**, 248–258 (2002).
81. Mossman, H. L., Brown, M. J. H., Davy, A. J. & Grant, A. Constraints on salt marsh development following managed coastal realignment: dispersal limitation or environmental tolerance? *Restor. Ecol.* **20**, 65–75 (2012).
82. Mossman, H. L., Davy, A. J. & Grant, A. Does managed coastal realignment create saltmarshes with 'equivalent biological characteristics' to natural reference sites? *J. Appl. Ecol.* **49**, 1446–1456 (2012).
83. Wolters, M., Garbutt, A., Bekker, R. M., Bakker, J. P. & Carey, P. D. Restoration of salt-marsh vegetation in relation to site suitability, species pool and dispersal traits. *J. Appl. Ecol.* **45**, 904–912 (2008).
84. Nicholls, R. J. et al. Stabilization of global temperature at 1.5°C and 2.0°C: implications for coastal areas. *Phil. Trans. A Math. Phys. Eng. Sci.* **376**, 20160448 (2018).
85. Song, J., Fu, X., Wang, R., Peng, Z.-R. & Gu, Z. Does planned retreat matter? Investigating land use change under the impacts of flooding induced by sea level rise. *Mitig. Adapt. Strategies Glob. Change* **23**, 703–733 (2017).
86. Sadoff, C. W. et al. *Securing Water, Sustaining Growth: Report of the GWP/OECD Task Force on Water Security and Sustainable Growth* (Univ. Oxford, Oxford, 2015).
87. Mittermeier, R. A. et al. Wilderness and biodiversity conservation. *Proc. Natl Acad. Sci. USA* **100**, 10309–10313 (2003).
88. Abel, N. et al. Sea level rise, coastal development and planned retreat: analytical framework, governance principles and an Australian case study. *Environ. Sci. Policy* **14**, 279–288 (2011).
89. Kousky, C. Managing shoreline retreat: a US perspective. *Clim. Change* **124**, 9–20 (2014).
90. Field, C. R., Dayer, A. A. & Elphick, C. S. Landowner behavior can determine the success of conservation strategies for ecosystem migration under sea-level rise. *Proc. Natl Acad. Sci. USA* **114**, 9134–9139 (2017).
91. The Organisation for Economic Co-operation and Development (OECD). *OECD Regional Typology* (OECD, Paris, 2011).



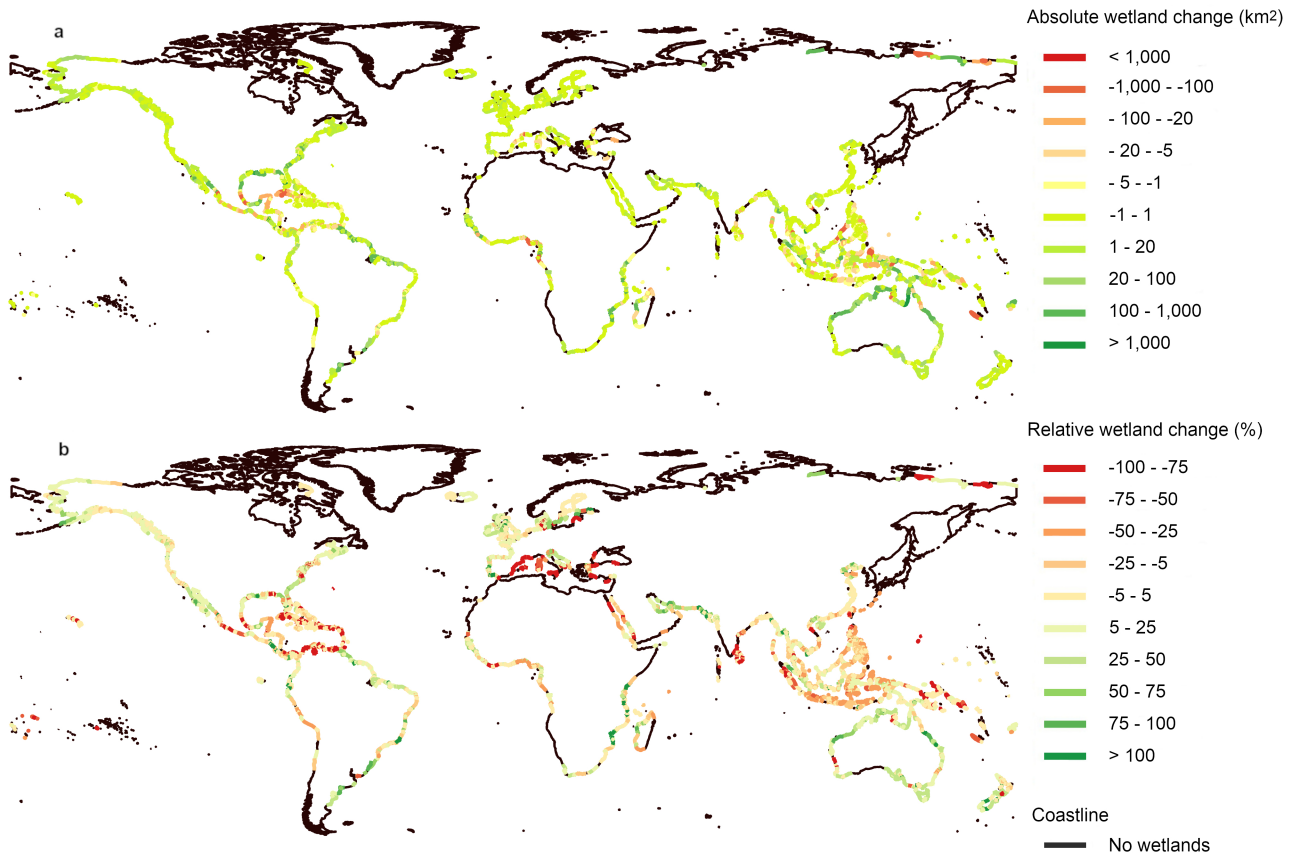
Extended Data Fig. 1 | Map of model performance during model calibration. Green lines indicate segments in which the modelled sediment balances match the observed trends in wetland elevation change relative to sea-level rise^{3,4,19}. Red segments indicate model mismatches. The frequency distributions for total suspended matter (TSM) and tidal range (TR) display the distributions of both parameters in matching

(green bars) and mismatching segments (red bars), and how they compare to the overall frequency distributions of both parameters (blue bars). The overall frequency distribution only includes coastline segments where coastal wetlands are present. The displayed coastline was generated during the DINAS-COAST FP5-EESD EU project (EVK2-CT-2000-00084).

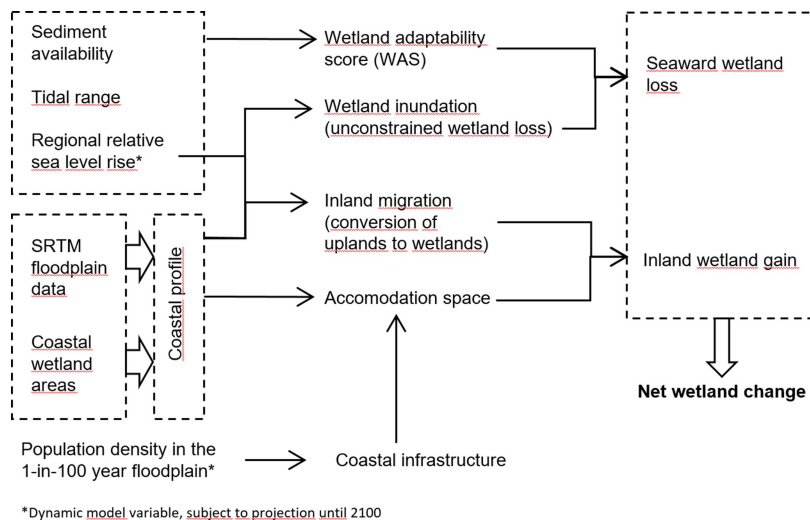


Extended Data Fig. 2 | Global change in coastal wetland area. Results for all three SLR scenarios (RCP 2.6, low; RCP 4.5, medium; RCP 8.5, high) and a total of eight different model configurations. These include the upper and lower boundaries of the BAU (5 and 20 people km⁻²) and the upper boundaries of the NB 1 and NB 2 scenarios (150 and 300 people

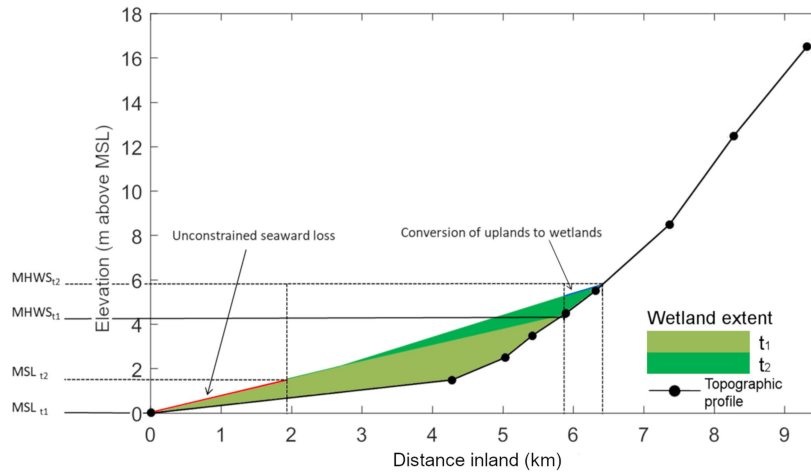
km⁻²) as defined in Extended Data Table 2 (solid lines). The dashed lines represent the four hypothetical scenarios, as characterized in Extended Data Table 2: (i) wetland migration only; (ii) sediment accretion only; (iii) maximum resilience; and (iv) no resilience.



is subject the population growth throughout the simulation period, following the Shared Socio-Economic Pathway SSP2^{20,68}. The displayed coastline was generated during the DINAS-COAST FP5-EESD EU project (EVK2-CT-2000-00084).

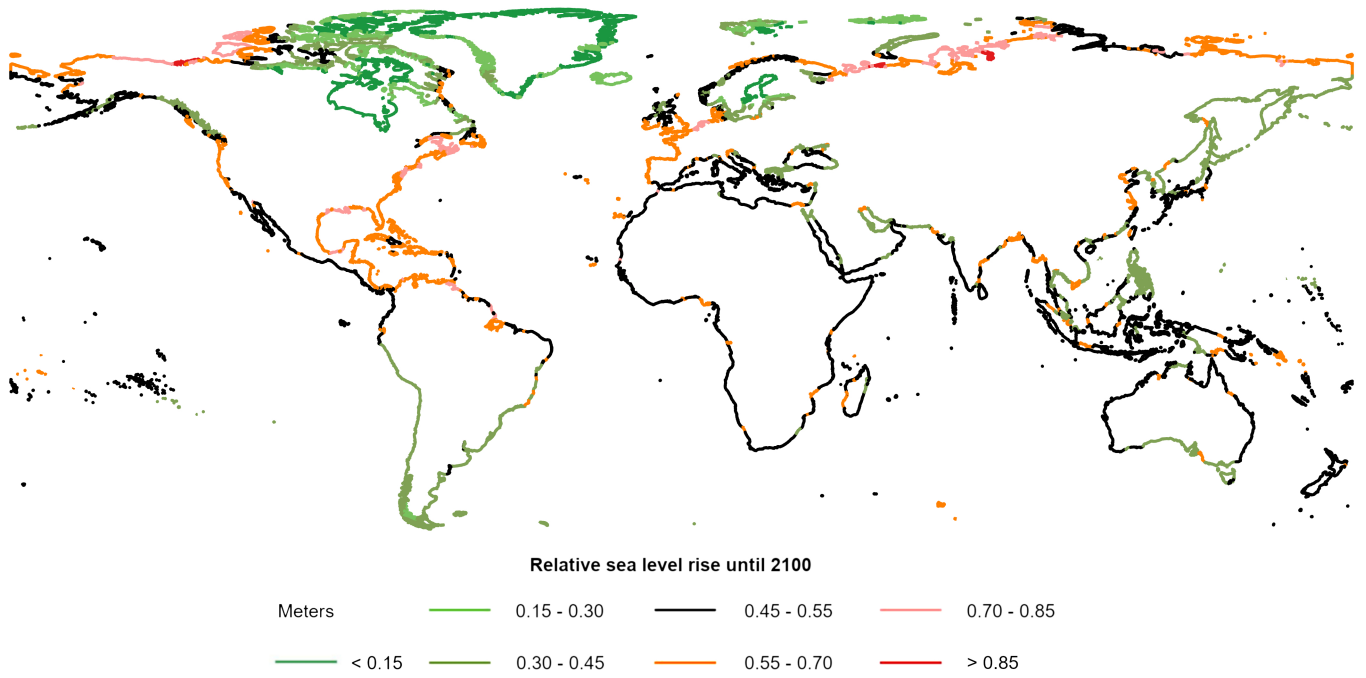


Extended Data Fig. 4 | Flow diagram representing the overall structure of the global coastal wetland model. Input parameters are shown on the left, output parameters are on the right. Net wetland change equals inland wetland gain minus seaward wetland loss.



Extended Data Fig. 5 | Schematization of topographic profiles. The conversion of upland areas to coastal wetlands (if not inhibited by anthropogenic barriers) and the unconstrained seaward loss of coastal wetlands in response to sea-level rise is shown for an exemplary coastline segment (in western France). Inundation of terrestrial uplands follows the

rising mean high water spring (MHWS) level between the time steps t_1 and t_2 (blue), whereas the unconstrained seaward loss follows the increase in mean sea level (MSL) when neglecting sediment accretion processes (red). To improve the clarity of the figure the actual MHWS level (2.54 m) and MSL rise are exaggerated.



Extended Data Fig. 6 | Map of regionalized relative sea-level rise. Total relative sea-level rise (in m) for the medium SLR scenario (Extended Data Table 2) during the simulation period, including a delta subsidence rate of 2 mm yr^{-1} (2010–2100). Black coastlines indicate regions of

relative sea-level rise similar to the global mean. The displayed coastline was generated during the DINAS-COAST FP5-EESD EU project (EVK2-CT-2000-00084).

Extended Data Table 1 | Performance of calibrated model when compared to field data

	Category (defined based on the field measurements)	Categorization of Field measurements	WAS	Model fit (number of segments)	Total occurrences (number of segments)
Tidal marshes	Total model fit	All data	All data	16	23
	"elevation deficit"	< -2 mm yr ⁻¹	<-1	3	5
	"balanced"	-2 to 2 mm yr ⁻¹	-1 to 1	10	10
	"elevation surplus"	> 2 mm yr ⁻¹	>1	3	8
Mangrove systems	Total model fit	All data	All data	20	23
	"elevation deficit"	< -2 mm yr ⁻¹	<-1	12	12
	"balanced"	-2 to 2 mm yr ⁻¹	-1 to 1	6	6
	"elevation surplus"	> 2 mm yr ⁻¹	>1	2	5

Summary of comparison between locally measured trends in surface elevation growth for tidal marshes^{3,4} and mangrove systems¹⁹ and modelled trends derived from the calculated WAS using $m_{TM} = 3.42$, $m_{Man} = 4.42$, $i_{TF} = -1.5$, $i_{Man} = 0$, $e_{TF} = 0.915$, $e_{Man} = 1.18$ and $a = 40 \text{ mg l}^{-1}$. 'Model fit' represents the number of segments, where the calculated WAS corresponds with the measured category for vertical wetland growth.

Extended Data Table 2 | Characteristics of the scenarios

SLR scenario	Land-ice contribution	SLR until 2100 (cm)	Accommodation space scenario		Scenario	Population density threshold (people km ⁻²)		Sediment accretion
						Lower boundary	Upper boundary	
Low: RCP 2.6 (5%)	low	29	Human adaptation scenarios	BAU*	BAU	5	20	Yes
				NB†	NB 1	20	150	
				NB†	NB 2	150	300	
			4 Hypothetical scenarios (HYS)	HYS 1	∞‡	∞‡	No	
				HYS 2	0§	0§	Yes	
				HYS 3	∞‡	∞‡	Yes	
				HYS 4	0§	0§	No	
Medium: RCP 4.5 (50%)	medium	50	Human adaptation scenarios	BAU*	BAU	5	20	Yes
				NB†	NB 1	20	150	
				NB†	NB 2	150	300	
			4 Hypothetical scenarios (HYS)	HYS 1	∞‡	∞‡	No	
				HYS 2	0§	0§	Yes	
				HYS 3	∞‡	∞‡	Yes	
				HYS 4	0§	0§	No	
High: RCP 8.5 (95%)	high	110	Human adaptation scenarios	BAU*	BAU	5	20	Yes
				NB†	NB 1	20	150	
				NB†	NB 2	150	300	
			4 Hypothetical scenarios (HYS)	HYS 1	∞‡	∞‡	No	
				HYS 2	0§	0§	Yes	
				HYS 3	∞‡	∞‡	Yes	
				HYS 4	0§	0§	No	

*BAU: Business-as-usual scenario

†NB: Nature-based adaptation scenarios

‡Population density threshold = ∞: Unlimited accommodation space

§Population density threshold = 0: No accommodation space

Three SLR scenarios (RCP 2.6, low; RCP 4.5, medium; RCP 8.5, high) were combined with three human adaptation scenarios (BAU; NB 1; and NB 2), accounting for varying degrees of accommodation space available for coastal wetlands, and four hypothetical scenarios (HYS 1: wetland migration only, HYS 2: sediment accretion only, HYS 3: maximum resilience, HYS 4: no resilience), used to quantify the contribution of vertical sediment accretion and horizontal inland migration to the overall resilience of coastal wetlands to global SLR (sensitivity analysis).

Extended Data Table 3 | Model sensitivity to variations in sediment availability

Human adaptation scenario	Population density threshold (people km ⁻²)	Sediment availability (constant in time)	RCP 2.6 - low (percent)	RCP 4.5 - medium (percent)	RCP 8.5 - high (percent)
Nature-based adaptation 2 – upper boundary	300	-50%	-2.9	-4.3	-6.5
		-20%	-1.1	-1.6	-2.5
		+20%	0.9	1.4	2.7
		+50%	2.5	3.5	6.1
Nature-based adaptation 2 – lower boundary = Nature-based adaptation 1 – upper boundary	150	-50%	-2.9	-4.3	-6.4
		-20%	-1.1	-1.6	-2.5
		+20%	0.9	1.4	2.7
		+50%	2.5	3.5	6.0
Nature-based adaptation 1 – lower boundary = Business-as-usual – upper boundary	20	-50%	-2.8	-4.1	-6.0
		-20%	-1.0	-1.5	-2.3
		+20%	0.9	1.3	2.5
		+50%	2.3	3.4	5.7
Business-as-usual – lower boundary	5	-50%	-2.7	-3.9	-5.7
		-20%	-1.0	-1.4	-2.2
		+20%	0.9	1.3	2.3
		+50%	2.3	3.3	5.3

Percentage deviations in total global wetland area by 2100 from simulations with current-day sediment availability for all four population density thresholds (Extended Data Table 2) and reductions/increases of the constant sediment supply by 50% and 20%.

Extended Data Table 4 | Model sensitivity to variations in natural and human-induced delta subsidence

Model setup	Delta subsidence (mm yr ⁻¹)	RCP 2.6 - 5% (percent)	RCP 4.5 - 50% (percent)	RCP 8.5 - 95% (percent)
Pop. density threshold 300	0	14.0	18.7	55.8
Pop. density threshold 150		11.4	14.8	39.5
Pop. density threshold 20		0.1	-1.0	-10.2
Pop. density threshold 5		-6.7	-10.6	-31.3
Pop. density threshold 300	2	15.2	19.8	59.7
Pop. density threshold 150		12.3	15.3	42.4
Pop. density threshold 20		0.2	-0.8	-7.6
Pop. density threshold 5		-7.6	-11.9	-30.3
Pop. density threshold 300	5	16.7	21.5	62.7
Pop. density threshold 150		12.8	15.5	44.1
Pop. density threshold 20		0.5	1.2	-6.3
Pop. density threshold 5		-9.6	-14.6	-31.0

Percentage gain (positive) and loss (negative) of total global wetland area by 2100 from simulations for all four population density thresholds (Extended Data Table 2) and three different rates for uniform delta subsidence for all 117 deltas listed in the DIVA database³¹.